

Fine interference fringes formed in high-order harmonic spectra generated by infrared driving laser pulses

Han Xu,¹ Hui Xiong,¹ Zhinan Zeng,¹ Yuxi Fu,^{1,2} Jinping Yao,^{1,2} Ruxin Li,¹ Ya Cheng,^{1,*} and Zhizhan Xu^{1,†}

¹State Key Laboratory of High Field Laser Physics, Shanghai Institute of Optics and Fine Mechanics, Chinese Academy of Sciences, Shanghai 201800, China

²Graduate University of Chinese Academy of Sciences, Beijing 100049, China

(Received 29 June 2008; published 30 September 2008)

We experimentally investigate the high-order harmonic generation in argon gas using a driving laser pulse at a center wavelength of 1240 nm. High-contrast fine interference fringes could be observed in the harmonic spectra near the propagation axis, which is attributed to the interference between long and short quantum paths. We also systematically examine the variation of the interference fringe pattern with increasing energy of the driving pulse and with different phase-matching conditions.

DOI: 10.1103/PhysRevA.78.033841

PACS number(s): 42.65.Ky, 42.65.Re

I. INTRODUCTION

High-order harmonic generation (HHG) has been intensively investigated for almost two decades since its discovery due to its potential applications as an intense, coherent, femtosecond to attosecond extreme ultraviolet (XUV) or soft-x-ray source [1–4] as well as a probe of molecular dynamics [5]. In a classical picture, HHG can be well understood as a three-step process which includes (1) tunnel ionization of an atom or a molecule in strong laser field; (2) acceleration of the free electron in an oscillating laser field in which the electron can be driven back toward its parent ion when the laser field changes its sign; and (3) recombination of the return electron and its parent ion by which the kinetic energy of the electron is released in the form of a harmonic photon [6]. From this picture, it can be found that for each order harmonic, it is mainly contributed by a pair of electron trajectories with the “long” trajectory corresponding to the electron ionized earlier (slightly after the peak of the laser electric field cycle) and the “short” one later in the same half-cycle. Although the photon energies of harmonics contributed by a pair of long and short trajectories are the same, the phases of the harmonic radiations are proportional to the classical action accumulated in the laser field, and are therefore very different [7,8]. Recently, the influence of the long and short trajectories on the spatial, temporal, and spectral structures of the HHG spectrum has attracted significant attention, whereas all the experiments were performed with Ti:sapphire laser sources at near-800-nm wavelengths [9–11]. As the atomic dipole phase φ_q in each quantum path of the q th-order harmonic is given by the ponderomotive energy $U_p(\sim\lambda^2)$ and electron traveling time $\tau_q(\sim\lambda)$, which could be written as $\varphi_q \approx -U_p\tau_q$ [11], the dipole phase accumulated in the longer wavelength driving field would be much larger because the electron could have higher ponderomotive energy and longer traveling time. It can be expected that more complicated roles could be played by the quantum trajectories at a longer [e.g., infrared (ir)] wavelength of the driving laser pulse. On the other hand, extending an attosec-

ond pulse into the keV range with ir laser field has also attracted much attention, but the influence of an ir pulse on the HHG process has not been fully experimentally studied [12,13]. In the last few years, thanks to the rapid development of ultrafast laser technology, high-power femtosecond optical parametric amplifiers (OPAs) which are able to offer intense ultrashort laser pulse at ir wavelengths for HHG have become commercially available [13–15]. In this paper, we present experimental evidence on the quantum path interference for HHG driven by a tunable ir light source.

II. EXPERIMENT

The experimental setup is shown in Fig. 1. The ir laser pulses are generated by a femtosecond OPA (TOPAS-C, Light Conversion, Inc.) pumped by a commercial Ti:sapphire laser system (Legend, Coherent, Inc.). The Ti:sapphire laser, operated at a repetition rate of 1 kHz, provides ~ 40 fs [full width at half-maximum (FWHM)] laser pulses with a central wavelength at 800 nm and a single pulse energy of ~ 2.5 mJ. The central wavelength of the signal pulse generated by OPA is fixed at 1240 nm, and the pulse duration (FWHM), measured by a home-made single-shot second-order autocorrelator (SSA), is approximately ~ 30 fs. By using dielectric coated broadband mirrors with high reflection coating at 1100 nm–1300 nm, only the signal pulse is chosen whereas the idler pulse centered at ~ 2300 nm is eliminated. After that, the signal pulse is focused by a fused silica lens with a focal length of 15 cm to achieve a peak intensity up to $\sim 1.5 \times 10^{14}$ W/cm² at the focus. The high-order harmonic emission is generated in a 4-mm-long gas cell filled with argon gas mounted within a vacuum chamber, and the pressure in the gas cell is set to be 51.1 mbar in this experiment. The HHG spectra are measured by a flat-field grating spectrometer equipped with a soft-x-ray CCD (Princeton Instruments, 1340 \times 400 imaging array PI: SX 400). A 500 nm thickness aluminum foil is placed at the entrance of the spectrometer to block the low-order harmonics. As the HHG signal is much weaker for ir the driving field, an integration time (6×10^4 shots) of ~ 1 min is performed to acquire a single HHG spectrum, and the fine structure of the spectrum could be well preserved due to the low-energy fluctuation of the OPA ($< 1\%$).

*ycheng-45277@hotmail.com

†zzxu@mail.shnc.ac.cn

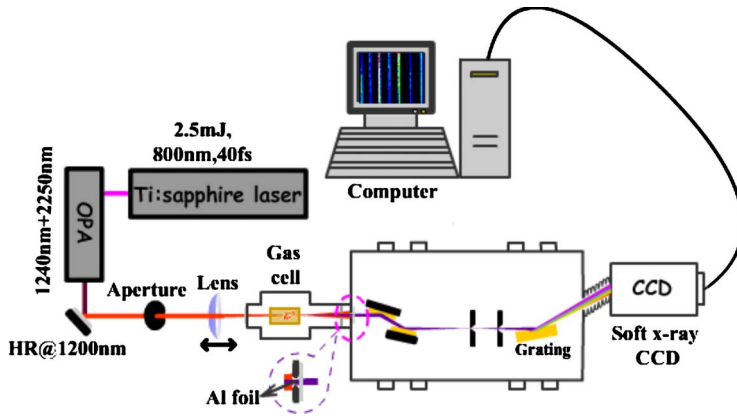


FIG. 1. (Color online) Experimental setup.

The input power of the ir pump beam could be smoothly tuned by continuously adjusting the size of the annular aperture placed before the focal lens. The focal lens is mounted on a translation stage to provide fine position adjustment along the propagation direction, so that the focus in the gas cell could be scanned in order to fulfill a phase-matching condition in favor of either the long or short electron trajectory.

III. RESULTS AND DISCUSSION

Figure 2 shows the HHG spectra obtained at different average powers of the OPA with the focus fixed about 4 mm

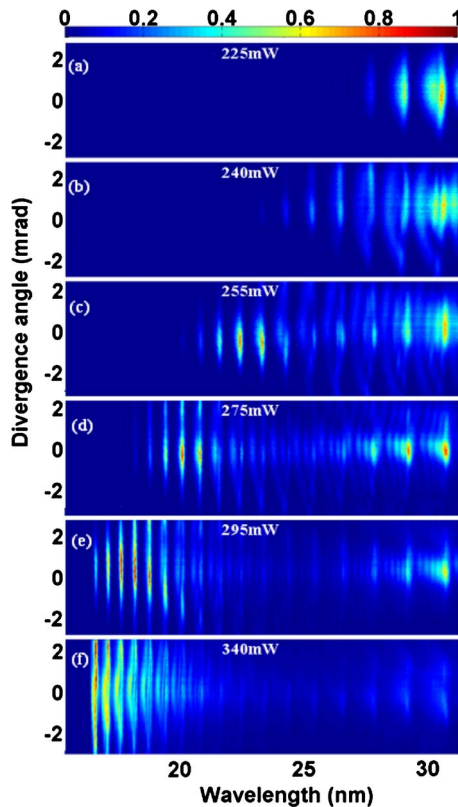


FIG. 2. (Color online) Normalized HHG spectra obtained at different powers of the ir driving source: (a) 225 mW; (b) 240 mW; (c) 255 mW; (d) 275 mW; (e) 295 mW; and (f) 340 mW.

after the center of the gas cell, where the spectral interference fringes are optimized for achieving the highest contrast. One can clearly see that as the laser power increases, the cutoff of HHG is continuously pushed toward high energy. This is consistent with the well-known HHG cutoff law $E_{\max} = I_p + 3.17U_p$ [6,7], where I_p denotes the binding energy of the target atom and ponderomotive energy is given by $U_p = E_L^2 / (4\omega^2)$ (E_L , laser electric field strength; ω , laser frequency). In addition, we observe broadening and formation of fine interference fringes in the HHG spectra. A general feature in Fig. 2 is that for high-order harmonics near the cutoff region, their spectra are relatively narrow compared to those in the plateau region, and all show a single-peak structure; whereas toward the plateau region, the spectra of low-order harmonics are significantly broadened, and clearly visible fine interference fringes are formed. The number of interference fringes increases as the harmonic order decreases. This interesting phenomenon could be attributed to the interference among long and short electron trajectories in the HHG process [9–11,16]. Generally speaking, interference among quantum trajectories could occur for harmonics generated either at the subcycle time scale (within a single half-optical cycle) or at different times of the laser envelope (in different half-cycles). However, as it has been shown in Ref. [17], interference among quantum trajectories which contribute simultaneously to a harmonic at a specific wavelength generated within different half-cycles can be ruled out in our experiment because of the random carrier-envelope phase of the driving pulse which will smear out these interference fringes. Consequently, only the first-order quantum path interference (QPI) is allowed to occur in our experiment [11]. Self-phase modulation in an ionized gas can also cause spectral splitting due to the distortion of the fundamental driving pulse [18,19]; however, the low peak intensities used in this experiment rule out such a possibility. It should be noted that the maximum energy of our ir driving pulse is $\sim 340 \mu\text{J}$, as shown in Fig. 2(f).

In comparison with the conventional 800-nm pump laser, the use of the ir driving field can promote the formation of high-contrast interference fringes in HHG spectra mainly due to the following reasons. First, for two optical pulses with different wavelengths but a same duration, the ir pulse is composed of less oscillation cycles than the 800-nm field with the same pulse duration. In this case, although the broadening of the HHG spectrum would remain the same,

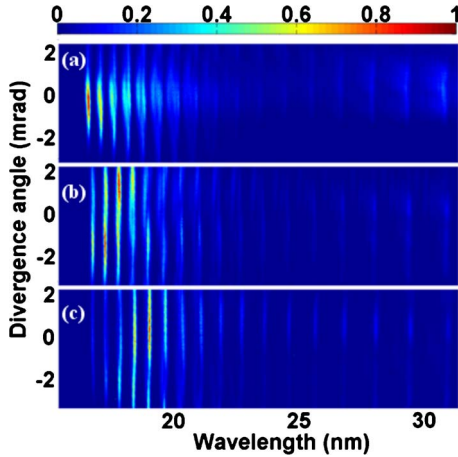


FIG. 3. (Color online) Normalized HHG spectra captured on CCD when the ir beam is focused (a) 6 mm after the center of the gas cell; (b) at the center of the gas cell; and (c) 2 mm before the center of the gas cell.

the spacing between the orders is closer. In addition, the bandwidth broadening of high-order harmonics is mainly originated from the chirp of harmonic emission induced by temporal variation of the dipole phase, which could be expressed as $\partial_t[\varphi(t)_q] \approx \alpha_q \partial_t I(t)$ [11], where α_q is roughly proportional to the electron traveling time and $I(t)$ is the temporal envelope of the driving field. As the electron traveling time is longer in the ir field, the frequency chirp and in turn the harmonic spectral bandwidth would also be increased. Both these two effects could facilitate an easy observation of the interference fringes on the HHG spectra. Second, we observe that the HHG emission has a smaller divergence angle with the ir driving field than with the 800 nm pump pulse, because the phase velocity difference between the driving pulse and the harmonic field actually decreases with the increasing wavelength of the pump pulse, so that the phase-matching condition can be fulfilled within a small divergence angle near the propagation axis. Due to this reason, we could improve the balance between the long and short trajectory contributions in both on-axis and off-axis areas by properly adjusting the phase-matching parameters in the experiment. In contrast, with an 800-nm-wavelength pump field, owing to the difficulty in realizing the on-axis phase matching for long trajectory HHG, high-contrast interference fringes could only appear in the off-axis area with large divergence angle [11]. Last, as shown in Fig. 2, the number of HHG interference fringes increases with the increasing pump power and decreasing harmonic order, which should be caused by the increasing dipole phase difference between the long and short trajectories as the pump laser intensity as well as the difference between the electron traveling times increases.

In Fig. 3, we show HHG spectra obtained at different focal positions with an average output power of the OPA at ~ 315 mW. In Figs. 3(a)–3(c), the focal spot is located ~ 6 mm after the center of the gas cell, at the center of the gas cell, and ~ 2 mm before the center of the gas cell, respectively. Thus, similar to HHG with a gas jet, we can selectively enhance the contribution from the short trajectory

by focusing the ir beam before the center of the gas cell, or enhance the contribution from the long trajectory by focusing the ir beam after the center of the gas cell [2]. Therefore, as we can see in Fig. 3, the HHG spectra are broadest in Fig. 3(a) because, in this case, the phase-matching condition preferentially selects the long trajectory. Due to the longer traveling time in the laser field, HHG spectra contributed by long trajectory are generally broader and more blueshifted than that contributed by the short trajectory [20]. When the focus is shifted to the center of the gas cell as shown in Fig. 3(b), the signal from the long trajectory is weakened, resulting in narrowed HHG spectra. The interference fringes show highest contrast in Fig. 3(b) owing to the balanced contributions from the long and short trajectories. Further moving the focus of ir beam before the center of the gas cell leads to sharpened HHG spectra in both cutoff and plateau regions as shown in Fig. 3(c), whereas the interference fringes are significantly blurred due to the changed phase-matching condition which now mainly selects the short trajectory. The sensitivity of HHG fringes to the focal position again strongly suggests that it is the interference between the quantum trajectories (e.g., the short and long trajectories) playing the dominant role behind this phenomenon.

IV. CONCLUSIONS

To conclude, we have experimentally investigated HHG in a gas cell filled with argon using an ir driving laser source. Fine interference fringes in HHG spectra caused by the interference between the long and short electron trajectories could be observed by properly adjusting the distance between the focal point and the center of the gas cell. The number of HHG interference fringes gradually increases with decreasing harmonic order and increasing pump intensity which is caused by the variation of the dipole phase difference between long and short trajectories; and the interference fringes are formed almost on-axis with a small divergence angle which indicates that phase-matching conditions of both long and short quantum trajectories could be simultaneously fulfilled along the propagation axis, i.e., the strongest harmonic intensity region. Our results indicate that the phase of harmonic emission could have a stronger influence on HHG spectra obtained by ir driving laser pulses than by traditional 800-nm driving pulses, largely owing to the extended electron traveling time in ir laser fields. Therefore, although it has been predicted by several groups that HHG yield will rapidly decrease as the wavelength of the driving laser pulse increases [21], inclusion of macroscopic propagation effects such as phase matching might greatly change this scenario and offer a potential solution [22].

ACKNOWLEDGMENTS

This research was supported by the National Basic Research Program of China (Grant No. 2006CB806000). Y.C. acknowledges the support of the 100 Talents Program of the Chinese Academy of Sciences, Shanghai Pujiang Program, and National Outstanding Youth Foundation.

- [1] P. Agostini and L. F. DiMauro, *Rep. Prog. Phys.* **67**, 813 (2004).
- [2] A. Scrinzi, M. Yu. Ivanov, R. Kienberger, and D. M. Villeneuve, *J. Phys. B* **39**, R1 (2006).
- [3] Z. Zeng, Y. Cheng, X. Song, R. Li, and Z. Xu, *Phys. Rev. Lett.* **98**, 203901 (2007).
- [4] P. Lan, P. Lu, W. Cao, Y. Li, and X. Wang, *Phys. Rev. A* **76**, 011402(R) (2007).
- [5] M. Lein, *J. Phys. B* **40**, R135 (2007).
- [6] P. B. Corkum, *Phys. Rev. Lett.* **71**, 1994 (1993).
- [7] M. Lewenstein, Ph. Balcou, M. Yu. Ivanov, A. L'Huillier, and P. B. Corkum, *Phys. Rev. A* **49**, 2117 (1994).
- [8] Y. Mairesse, A. de Bohan, L. J. Frasinski, H. Merdji, L. C. Dinu, P. Monchicourt, P. Breger, M. Kovačev, R. Taïeb, B. Carré, H. G. Muller, P. Agostini, and P. Salières, *Science* **302**, 1540 (2003).
- [9] E. Brunetti, R. Issac, and D. A. Jaroszynski, *Phys. Rev. A* **77**, 023422 (2008).
- [10] M. Bellini, C. Lyngå, A. Tozzi, M. B. Gaarde, T. W. Hänsch, A. L'Huillier, and C.-G. Wahlström, *Phys. Rev. Lett.* **81**, 297 (1998).
- [11] A. Zaïr, M. Holler, A. Guandalini, F. Schapper, J. Biegert, L. Gallmann, U. Keller, A. S. Wyatt, A. Monmayrant, I. A. Walmsley, E. Cormier, T. Augustine, J. P. Caumes, and P. Salières, *Phys. Rev. Lett.* **100**, 143902 (2008).
- [12] B. Shan and Z. Chang, *Phys. Rev. A* **65**, 011804(R) (2001).
- [13] P. Colosimo, G. Doumy, C. I. Blaga, J. Wheeler, C. Hauri, F. Catoire, J. Tate, R. Chirila, A. M. March, G. G. Paulus, H. G. Muller, P. Agostini, and L. F. DeMauro, *Nat. Phys.* **4**, 386 (2008).
- [14] H. Xu, H. Xiong, R. X. Li, Y. Cheng, Z. Z. Xu, and S. L. Chin, *Appl. Phys. Lett.* **92**, 011111 (2008).
- [15] H. Xiong, H. Xu, Y. Fu, Y. Cheng, Z. Xu, and S. L. Chin, *Phys. Rev. A* **77**, 043802 (2008).
- [16] M. B. Gaarde and K. J. Schafer, *Phys. Rev. A* **65**, 031406(R) (2002).
- [17] G. Sansone, E. Benedetti, J.-P. Caumes, S. Stagira, C. Vozzi, S. De Silvestri, and M. Nisoli, *Phys. Rev. A* **73**, 053408 (2006).
- [18] Y. Tamaki, J. Itatani, Y. Nagata, M. Obara, and K. Midorikawa, *Phys. Rev. Lett.* **82**, 1422 (1999).
- [19] Y. Wang, Y. Liu, X. Yang, and Z. Xu, *Phys. Rev. A* **62**, 063806 (2000).
- [20] H. J. Shin, D. G. Lee, Y. H. Cha, J.-H. Kim, K. H. Hong, and C. H. Nam, *Phys. Rev. A* **63**, 053407 (2001).
- [21] J. Tate, T. Augustine, H. G. Muller, P. Salières, P. Agostini, and L. F. DiMauro, *Phys. Rev. Lett.* **98**, 013901 (2007).
- [22] V. S. Yakovlev, M. Ivanov, and F. Krausz, *Opt. Express* **15**, 15351 (2007).